processes

*Article*

# A New Method for Numerical Simulation of Coalbed Methane Pilot Horizontal Wells—Taking the Bowen Basin C Pilot Area in Australia as an Example

**Xidong Wang [1], Lijiang Duan [2,*], Songhang Zhang [1,*], Shuheng Tang [1], Jianwei Lv [1] and Xudong Li [1]**

[1] School of Energy, China University of Geosciences, Beijing 100083, China; 18232462327@163.com (X.W.); tangsh@cugb.edu.cn (S.T.); lvjianwei618@163.com (J.L.); 17504852008@163.com (X.L.)
[2] PetroChina Research Institute of Petroleum Exploration & Development, Beijing 100083, China
* Correspondence: duanlj@petrochina.com.cn (L.D.); zhangsh@cugb.edu.cn (S.Z.)

**Abstract:** Coalbed methane (CBM) pilot wells typically exhibit a short production period, necessitating evaluation of their estimated ultimate recovery (EUR) through numerical simulation. Utilizing limited geological data from the pilot areas to finish history matching and subsequent production forecasting presents substantial challenges. This paper introduces a comprehensive numerical simulation workflow for CBM pilot wells, encompassing the following steps. Initially, geological parameters are categorized into two groups based on their statistical distribution trends: trend parameters (i.e., gas content, permeability, Langmuir volume, and Langmuir pressure) and non-trend parameters (i.e., fracture porosity, gas–water relative permeability, and rock compressibility). The probability method is employed to ascertain the probable high and low limits for trend parameter distributions, while empirical or analogous methods are applied to define the boundaries for non-trend parameters. Subsequently, the parameter sensitivity analysis is conducted to understand the influence of varying parameters on cumulative gas and water production. Conclusively, experimental design algorithms generate over 100 simulation cases using the identified sensitive parameters, from which the top ten optimal cases are chosen for EUR prediction. This workflow features two technological innovations: (1) considering the most comprehensive set of reservoir parameters for uncertainty and sensitivity analyses, and (2) considering the matching accuracy of both cumulative production and dynamic production trends when selecting optimal matching cases. This approach was successfully implemented in the C pilot area of the Bowen Basin, Australia. In addition, it offers valuable insights for numerical simulation of unconventional natural gases, such as shale gas.

**Keywords:** CBM pilot well; history matching; uncertainty analysis; sensitivity analysis

check for updates

**Citation:** Wang, X.; Duan, L.; Zhang, S.; Tang, S.; Lv, J.; Li, X. A New Method for Numerical Simulation of Coalbed Methane Pilot Horizontal Wells—Taking the Bowen Basin C Pilot Area in Australia as an Example. *Processes* **2024**, *12*, 616. https://doi.org/10.3390/pr12030616

Academic Editor: Raymond Cecil Everson

Received: 19 February 2024
Revised: 14 March 2024
Accepted: 16 March 2024
Published: 20 March 2024

**Copyright:** © 2024 by the authors. Licensee MDPI, Basel, Switzerland. This article is an open access article distributed under the terms and conditions of the Creative Commons Attribution (CC BY) license (https://creativecommons.org/licenses/by/4.0/).

## 1. Introduction

Pilot wells are essential in exploring and developing coalbed methane (CBM) resources [1]. Their primary purpose is to gather detailed information about the characteristics of CBM reservoirs and to test whether these reservoirs can produce CBM at commercial rates. Early geological understandings can also be updated through history matching of production data from pilot wells [2]. However, the production duration of pilot wells is typically short, and relevant geological data are usually scarce. These two factors pose challenges in selecting suitable methods for numerical simulation [3].

History matching serves as a critical intermediary between geological model construction and production forecasting [4]. It refines the reservoir parameters of static geological models by aligning them with dynamic production data, thereby establishing a solid foundation for subsequent production predictions. Generally, history matching methods for pilot wells fall into two categories: the manual trial-and-error (MTE) method and the experimental design (ED) method [5]. The MTE approach requires operators to manually adjust coal reservoir parameters to align with production data. Several international software platforms, such as Petrel RE 2023 and SIMEDWin, facilitate history matching. Nevertheless, core tasks, including parameter selection, modification sequence, and adjustment magnitude, remain predominantly manual. Scholars have primarily focused on parameter adjustments to optimize matching accuracy [6,7], addressing factors such as permeability, gas content, relative permeability of water and gas, Langmuir volume (VL), Langmuir pressure (PL), and fracture porosity [8–11]. However, research on the direction and extent of parameter adjustments is somewhat limited, and the methods applied are often arbitrary.

The ED method emerged in the industrial literature in the 1970s [12]. Currently, these techniques have been successful applied in underground uncertainty assessments [13,14], reserve estimation, and production forecasting [15]. Although several studies present practical applications, few specifically focus on applying the ED method to the numerical simulation of pilot wells [16]. The ED method typically involves two steps. The first involves selecting an ED algorithm (e.g., Box–Behnken, Central Composite) to generate various parameter combinations, establishing the upper and lower limits for each parameter, and creating simulation cases. The second step entails running these simulation cases and selecting the optimal matching cases based on parameter combinations. Using this approach, Alessio et al. [17] selected seven reservoir parameters and generated 28 matching cases for 11 wells in the F6 field in 2005 to assess the development risks; Zhao et al. [18] calibrated seven parameters, including permeability, gas content, VL, fracture porosity, rock compressibility, sorption time, and PL, and generated 77 simulation cases by selecting the six most sensitive parameters. The optimal simulation cases were chosen based on the matching results at the well group level; Duan et al. [1] utilized five parameters (i.e., permeability, gas content, fracture porosity, gas saturation, and variogram length) for history matching, generating 43 simulation cases through the ED method. Twenty top cases were identified based on the matching results of cumulative gas and water production in the single well level, and the intersection of these two results was determined as the optimal simulation cases for the entire well group.

Through the above discussion about simulation methods, it becomes apparent that using ED methods to generate multiparameter combinations is more appropriate for the history matching of the pilot wells [1,18–20]. This study introduces a comprehensive numerical simulation workflow for CBM wells, integrating the strengths of the aforementioned studies. Nine reservoir parameters are selected to enhance the comprehensiveness and representativeness of the parameters. Following uncertainty and sensitivity analyses, seven parameters are chosen, resulting in 143 simulation cases. In selecting the optimal simulation cases for the single well, the matching results of both the cumulative production and the dynamic production trends are considered. Initially, the best matching cases for gas and water in the single well level are identified, followed by determining their intersection to ensure applicability across all wells. This approach was successfully applied in the simulation work of the C pilot area in the Bowen Basin, Australia, and satisfying results were achieved.

## 2. Pilot Well Overview

### *2.1. Geological Background*

The Bowen Basin, a backarc foreland basin, is situated in Queensland, Australia, and extends southward into northern New South Wales. This asymmetric syncline spans approximately $0.2 \times 10^6$ km$^2$. Its two flanks feature differing syncline structures; the eastern flank is steeper and endures nearly east–west compressive stress, aligning predominantly with NNW [21] (Figure 1).

In the Bowen Basin, the Late Permian Blackwater Formation, deposited by river–lake facies, constitutes the primary coal-bearing strata. These strata evolve into a delta sedimentary system towards the south, reaching a total thickness of about 150 m. Three coal measures, namely the Rangal coal measures (RCM), Fort Cooper coal measures (FCCM), and Moranbah coal measures (MCM), are developed from top to the bottom. The target RCM primarily consists of siltstone, sandstone, interbedded mudstone, and coal seams.

It can be subdivided into 12 sublayers based on their sedimental cycles [18]. The coal seam thickness varies from 3.8 m to 26.9 m, averaging about 4 m. Its maximum vitrinite reflectance mainly varies from 1.2% to 1.8% [18,22]. The RCM is characterized by complex structures, thin coal seams, moderate gas content, high permeability, inactive groundwater, and localized crack development.

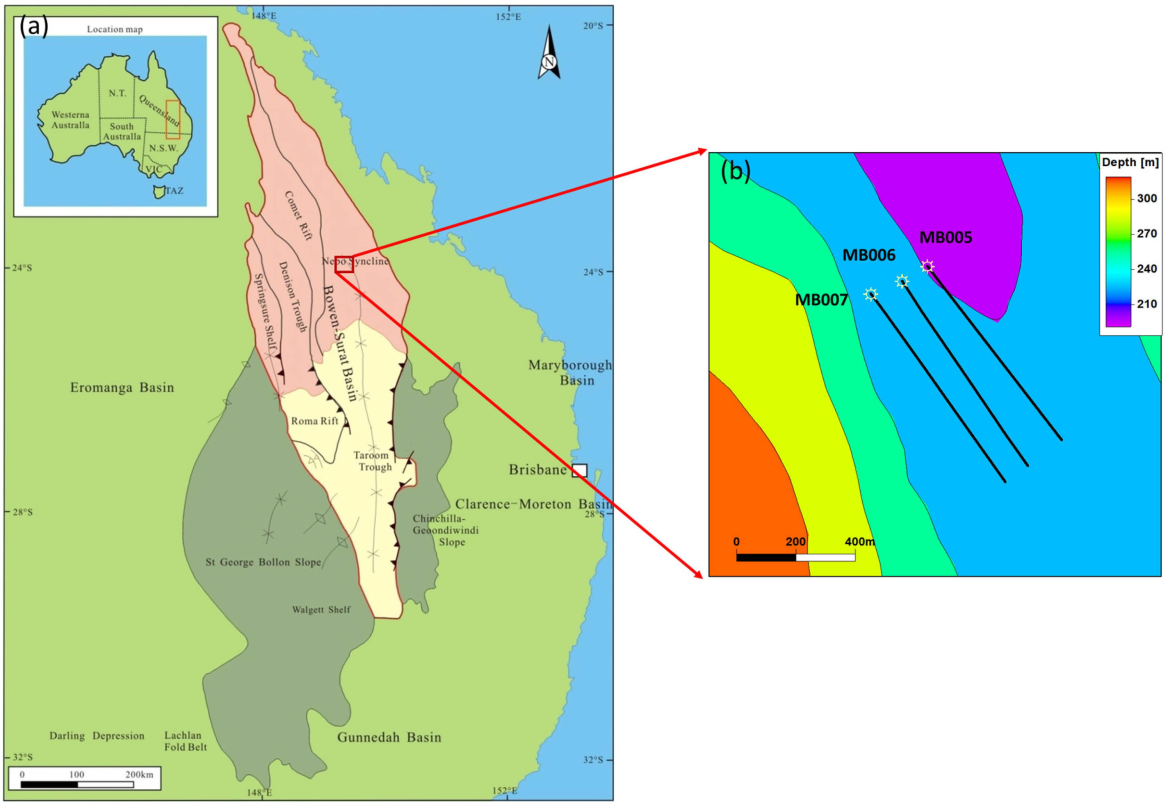


**Figure 1.** (**a**) Outline of Bowen Basin structure and (**b**) coal depth contour in the C pilot area.

The C pilot area lies on the eastern flank of the Nebo syncline [23], targeting a coal depth of 333 m to 346 m, averaging 342 m. In this area, the target coal thickness ranges from 4.3 m to 10.2 m, averaging 6.45 m. Three single lateral surface-into-seam (SIS) wells were drilled with a production period of about seven months.

## 2.2. Characteristics of CBM Reservoirs

Around the pilot area, 565 core samples from 45 wells were tested for gas content, ash content, VL, and PL. The measured dry ash-free gas content (GC_DAF) is 2.28 $m^3/t$ to 24.31 $m^3/t$, averaging 13 $m^3/t$; the ash content varies from 7% to 51.2%, with an average value of 21.1%. The measured VL ranges from 8.26 $m^3/t$ to 25.44 $m^3/t$, averaging 18.6 $m^3/t$, and the PL ranges from 1.76 MPa to 1.98 MPa, averaging 1.84 MPa. Due to the insufficiency of collected data and the high heterogeneity of the coal, although some correlation coefficients are not very strong, they still exhibit discernible trends [24] (Figure 2). The tested rock compressibility lies between $1 \times 10^{-5}$ $bar^{-1}$ and $3 \times 10^{-4}$ $bar^{-1}$, averaging $1.25 \times 10^{-4}$ $bar^{-1}$. The tested sorption time varies from 15 days to 89 days. Permeability data, sourced from on-site tests such as the drill stem test and diagnostic fracture injection test, range from 0.01 mD to 141.3 mD, averaging 15 mD.

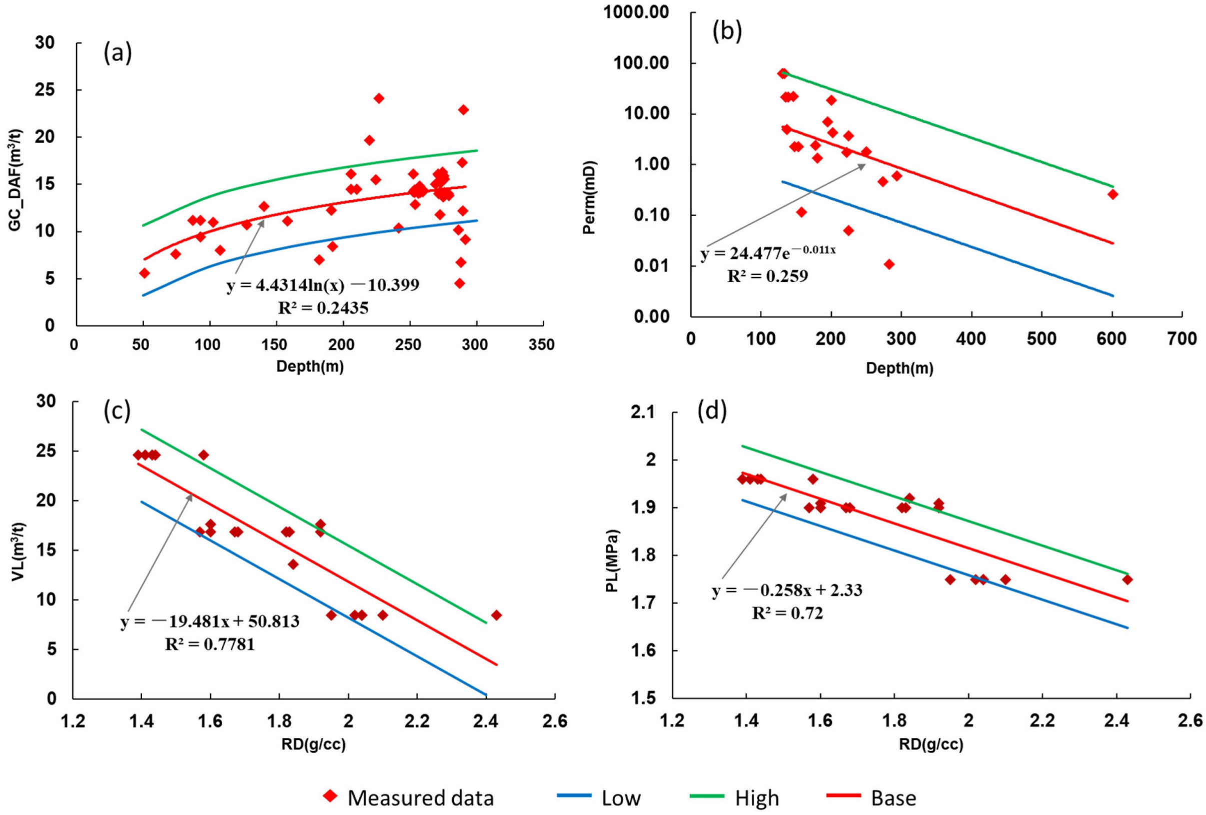


**Figure 2.** (**a**) Relationship between GC_DAF and burial depth, (**b**) relationship between permeability and burial depth, (**c**) relationship between VL and RD, and (**d**) relationship between PL and RD.

*2.3. Production Characteristics of Pilot Wells*

Figure 3 illustrates the production curves of three pilot wells, spanning a production period of seven months. Peak gas production varies from 12,470 $m^3$/d to 22,315 $m^3$/d, averaging 17,681 $m^3$/d (Figure 3a). Simultaneously, water production fluctuates from 42 $m^3$/d to 50 $m^3$/d, averaging 45.1 $m^3$/d (Figure 3b). Over these seven months, gas production has exhibited a continuous increase, characterized by a rapid growth rate in the initial two months and a consistent rise in subsequent months. In contrast, the water production demonstrates a decreasing trend, with the rate of decline diminishing in the later stages.

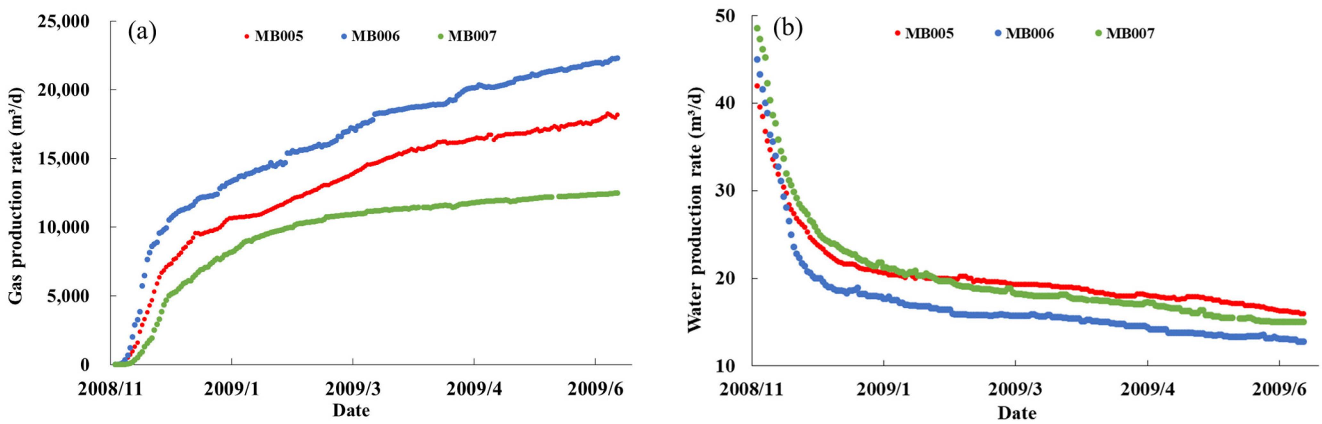


**Figure 3.** (**a**) Gas production profiles and (**b**) water production profiles.

## 3. Numerical Simulation Workflow

The CBM simulation is a crucial tool for detecting and predicting the flow dynamics of CBM within coal reservoirs. This method involves applying mathematical models and computational techniques to investigate the mechanisms of CBM storage, migration, and extraction. This study focuses on three CBM wells in the C pilot area of the Bowen Basin, Australia. The methodology is outlined in Figure 4. A manageable-sized model was extracted from the regional geo-model of the Bowen Basin. The selected model size balances computational efficiency and representativeness. Following quality control, production data from the pilot wells are loaded. After initializing the model, a thorough uncertainty analysis is conducted on nine parameters to enhance model accuracy and reliability. This analysis categorizes parameters into deterministic and indeterminate types (including both trend parameters and non-trend parameters), applying probabilistic methods to ascertain the upper and lower limits of trend parameters. Non-trend parameters are assigned values through empirical and analogical approaches. Subsequently, 18 simulation cases are generated, and these cases are run using a fixed bottom-hole flow pressure (BHFP) method. Each case's cumulative gas and water outputs are compared to those of the base case to identify sensitive parameters and create tornado plots.

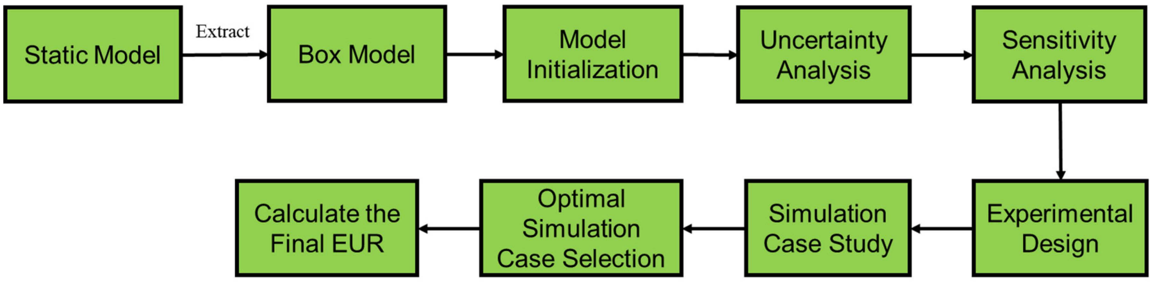


**Figure 4.** Numerical simulation workflow of CBM pilot well.

The matching parameters are ultimately selected based on the uncertainty and sensitivity analysis results of the reservoir parameters. These are then integrated as variables into the ED workflow. Utilizing the central composite sampler algorithm, over 100 simulation cases are generated, ensuring that the dynamic trends of gas and water production in each pilot well closely align with actual production dynamics. The simulations aim to achieve a congruent cumulative gas and water production. The study involves analyzing production characteristics, calculating the simulation deviation of cumulative gas and water production, and selecting the top ten simulation cases. Probability-based estimated ultimate recovery (EUR) predictions are formulated based on these selections. As the primary focus of this study is on numerical simulation, subsequent paragraphs will illustrate this from the stage of model initialization.

## 4. Preparation before Numerical Simulation

### *4.1. Dynamic Model Initialization*

The box model of the C pilot area is extracted from the regional geological model of the Bowen Basin, encompassing an area of 25 km$^2$ (5 km $\times$ 5 km). It includes nine vertical coal seams with a total thickness of 38 m. The planar grid features a uniform step size, with each grid measuring 100 m $\times$ 100 m. The total number of grids is 285,768 (126 $\times$ 126 $\times$ 18).

Reservoir parameters for dynamic model initialization generally fall into two categories: deterministic parameters and indeterminate parameters [25]. Deterministic parameters are known for their high reliability and are not modified in the history matching process. These include structure, initial conditions, PVT parameters, and capillary pressure. Conversely, indeterminate parameters represent unknown or uncertain elements in the history matching process. Depending on their statistical distribution patterns, these parameters are further classified into trend parameters and non-trend parameters [25].

Trend parameters, calculable by establishing correlations with other variables, encompass gas content, permeability, VL, and PL. Non-trend parameters, typically assigned based on empirical methods or analogies to other CBM gas fields in the Bowen Basin, include fracture porosity, gas–water relative permeability, rock compressibility, and sorption time (Table 1).

**Table 1.** Numerical simulation parameter classification.

| Indeterminate Parameters | | Deterministic Parameters |
| --- | --- | --- |
| **Trend Parameters** | **Non-Trend Parameters** | |
| Gas content | Fracture porosity | Structure |
| Permeability | Gas–water relative permeability | Initial conditions |
| VL | Rock compressibility | PVT parameters |
| PL | Sorption time | Capillary pressure |

The four trend parameters used in the box model of the pilot wells were derived from the regional geo-model of the Bowen Basin. The gas content is crucial for estimating the gas initially in place (GIIP). An examination of the GC_DAF data within the model reveals a correlation with depth, describable via a logarithmic equation. Permeability, pivotal in controlling coal reservoir fluid flow capacity and influencing the economic viability of CBM well development [26,27], is represented by an exponential equation relating permeability to depth. The isothermal adsorption curve is described by the Langmuir equation, which includes two key parameters, i.e., VL and PL. When predicting the distribution of VL and PL, a correlation with RD is established, respectively. The gas–water relative permeability of coal is a function of the saturation during the corresponding phase of the two-phase flow. When integrated with permeability data, it yields the effective permeability. In the dynamic model, relative permeability data are derived from Corey-type equations [28].

It should be noted that during the CBM developing process, permeability undergoes significant changes due to coal matrix shrinkage caused by decreasing reservoir pressure and coal matrix swelling caused by gas desorption. This process is simulated by the improved P & M model [29].

Five non-trend parameter settings in the box model of pilot wells are assigned values through empirical analysis and analogy. These settings include a fracture porosity of 0.4%, a rock compression coefficient of $5 \times 10^{-5}$ bar$^{-1}$, Corey coefficients for gas and water of 3 for both, and a sorption time of 50 days [5,18]. The aforementioned parameters represent the initial medium values in the dynamic model, as listed in Table 2.

**Table 2.** Dynamic model parameter setting of the pilot wells.

| Parameters | Low | Medium | High |
| --- | --- | --- | --- |
| Gas content (m$^3$/t) | $4.43 \times$ Ln(depth) $- 14.10$ | $4.43 \times$ Ln(depth) $- 10.39$ | $4.43 \times$ Ln(depth) $- 6.68$ |
| Permeability (mD) | $1.96 \times$ Exp($-0.011 \times$ depth) | $24.47 \times$ Exp($-0.011 \times$ depth) | $275.26 \times$ Exp($-0.011 \times$ depth) |
| VL (m$^3$/t) | $-19.48 \times$ RD $+ 47.17$ | $-19.48 \times$ RD $+ 50.81$ | $-19.48 \times$ RD $+ 54.45$ |
| PL (MPa) | $-0.258 \times$ RD $+ 2.275$ | $-0.258 \times$ RD $+ 2.33$ | $-0.258 \times$ RD $+ 2.388$ |
| Fracture porosity (%) | 0.1 | 0.4 | 1 |
| Corey gas | 2 | 3 | 4 |
| Corey water | 2 | 3 | 4 |
| Rock compressibility (bar$^{-1}$) | $1 \times 10^{-5}$ | $5 \times 10^{-5}$ | $5 \times 10^{-4}$ |
| Sorption time (days) | 10 | 50 | 100 |

In addition to the aforementioned nine reservoir parameters, drilling and completion and production data for the pilot wells were imported into the simulator after undergoing data quality control to initialize the dynamic model. The simulation cases employs the BHFP as the constraint to match the observed gas and water production data.

The study utilized the CBM module in Petrel RE 2023 software for conducting history matching, and the simulation process was governed by the material balance equation [5].

### 4.2. Parameter Uncertainty Analysis

#### 4.2.1. Analysis of Uncertainty in Trend Parameters

Gas content is typically determined through experimental analysis of coal cores obtained from drilling. Gas content is mainly influenced by coal rank, ash content, and maceral composition. A correlation of GC_DAF and depth is used in this study to predict the distribution of gas content, and scattered data points are found around the matching curve. In order to capture these uncertainties, the probability method is employed to ascertain the probable high and low limits, and the steps are described below. Firstly, the residuals between the measured values and corresponding values derived from the correlation equation are calculated separately. Following residual distribution analysis, the 90th and 10th percentile values are selected to delineate high and low trends, encompassing the majority of data points within the low-trend and high-trend bands (Figure 2a).

The permeability values show an exponentially decreasing trend with increasing burial depth. In the scope of the regional geo-model, permeability testing data are scarce and show significant variability, resulting in high uncertainty. The probability method is also used to draw the 90th and 10th percentile trends (Figure 2b).

Despite limited isothermal data availability, strong correlations exist for both VL vs. RD and PL vs. RD. In order to represent coal heterogeneity and the uncertainty arising from limited testing data [30], probability trends are established when predicting both the VL and PL distribution (Figure 2c,d).

#### 4.2.2. Analysis of Uncertainty in Non-Trend Parameters

Porosity is associated with the water storage capacity of reservoirs [31]. The Petrel RE 2023 software offers a dual-porosity model, ideal for the numerical simulation of CBM, encompassing both fracture porosity and matrix porosity. In other words, the fracture porosity in the dynamic model is a matching parameter, which has the highest uncertainties. Based on the rule-of-thumb, the high and low fracture porosity values are set as 1% and 0.1%, respectively.

The gas–water relative permeability used in the dynamic model is derived from the Corey equation rather than the measured values [32], resulting in high uncertainty. Analogous with the model setting of the CBM gas field in the Bowen Basin, the high and low Corey equation exponents were defined as 4 and 2 separately for gas and water.

The rock compression coefficient, denoting the volumetric shrinkage of rock under unit formation pressure, predominantly impacts reservoir permeability during the dewatering in CBM wells [33]. Due to the inadequate amount of testing data and high coal heterogeneity, the rock compressibility values are obtained by analogy, setting them at $5 \times 10^{-4}$ bar$^{-1}$ and $1 \times 10^{-4}$ bar$^{-1}$ for high and low estimates, respectively.

The sorption time values are tested from the desorption experiment of coal cores [34], which have a moderate uncertainty. For sorption time, the high and low values are set as 100 days and 10 days, respectively.

### 4.3. Parameter Sensitivity Analysis

In order to analyze the impact of reservoir parameter variations on cumulative gas and water production during the history matching process, a sensitivity analysis is conducted on the high, medium, and low values of the nine parameters. Initially, a base case is generated using medium values for each parameter. Subsequently, 18 simulation cases are established, adjusting only one parameter to its high or low value in each case while keeping the others at their median values. The final step involves comparing the calculated cumulative water and gas production from each simulation case with that of the base case. These comparisons are quantified by production deviation (PD) and sensitivity index (SI), which are defined as follows:

$$\mathrm{PD}\% = \frac{Q_s - Q_b}{Q_b} \times 100\% \tag{1}$$

$$\mathrm{SI} = PD_p - PD_n \tag{2}$$

where $Q_s$ is the simulated cumulative water or gas yield of the sensitive case ($m^3$); $Q_b$ is the simulated cumulative yield corresponding to the base case ($m^3$); $PD_p$ is the positive yield deviation of one parameter (%); and $PD_n$ is the negative yield deviation of the corresponding parameter (%).

As shown in Figure 5, the SI value for gas decrease in the parameter sequence of gas content, permeability, VL, fracture porosity, Corey gas, compressibility, Corey water, sorption time, and PL, and the SI value for water decrease in the parameter sequence of permeability, porosity, Corey water, Corey gas, VL, compressibility, gas content, PL, and sorption time.

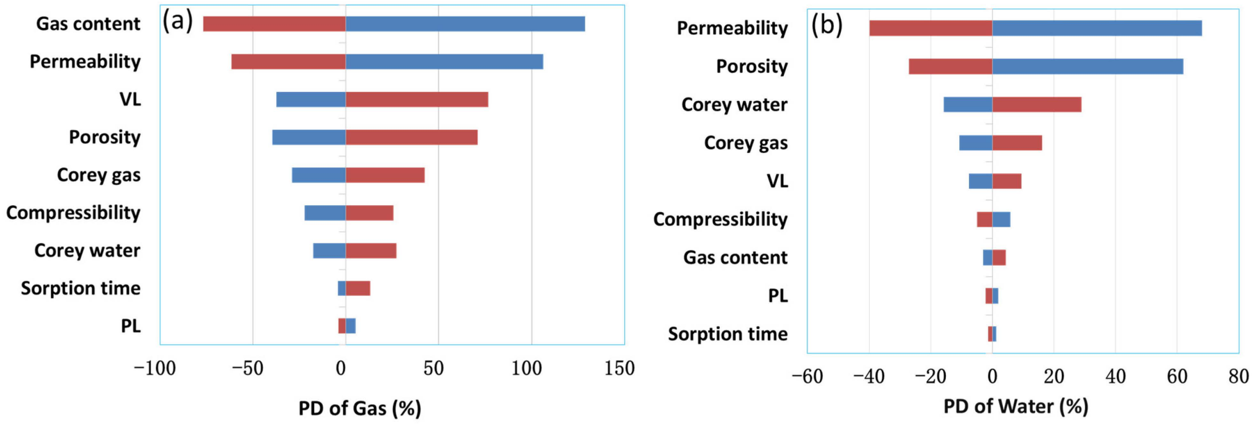


**Figure 5.** Tornado plots of the: (**a**) PD for gas and (**b**) PD for water (the blue bar indicates the high value of the parameter, and the red bar indicates the low value of the parameter).

Given the distribution of the SI values and the rules-of-thumb, 20% and 5% are selected as the threshold values for distinguishing sensitive parameters from non-sensitive parameters for gas and water, respectively. Because PL and sorption time are not sensitive to gas and water production, these two parameters are not considered in the following ED analysis.

Compared to the study of Zhao et al. [18], this paper incorporates an additional parameter, PL, which is used as a trend parameter, leading to a more comprehensive parameter setting. Duan et al. [1] utilize the variogram length in their research, which is less sensitive to production; thus, it is not employed in this study. Additionally, their study incorporates the concept of gas saturation, the ratio of gas content to the theoretical maximum adsorption capacity (calculated by VL and PL) under actual reservoir pressure. However, only three gas saturation values are assigned, inadequately describing the actual distribution of gas saturation under geological conditions. In other words, the parameter selection in this study is more reasonable.

## 5. Numerical Simulation Process

### *5.1. Simulation Cases Generation and Analysis*

Based on the sensitivity analysis results in the previous section, seven sensitive parameters are selected and input into the ED workflow as uncertain variables. The central composite sampling algorithm is employed for sampling and calculating uncertain parameters in their corresponding uncertainty ranges. And then, 143 simulation cases are generated and run for three pilot wells. Each case represents an optimized combination of low, medium, and high values for the seven parameters mentioned above.

Taking MB006 as an example, the observed production data are encompassed within the simulated curves of 143 generated cases. The simulated peak gas rate of the cases ranges from 4971 $m^3$/d to 40,722 $m^3$/d, with an average of 24,102 $m^3$/d. The simulated peak water rate of the cases ranges from 3.02 $m^3/d$ to 26.85 $m^3/d$, with an average of 14.93 $m^3/d$ (Figure 6a,c).

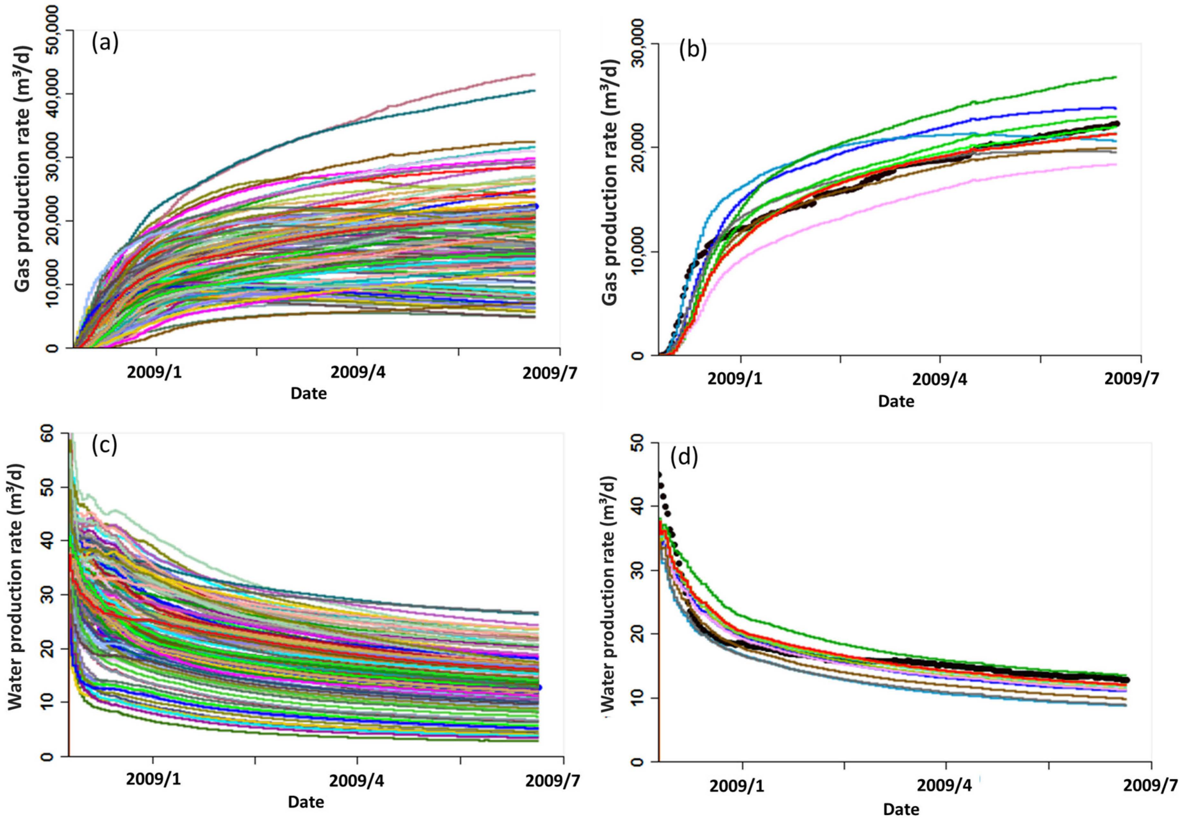


**Figure 6.** Gas rate matching results of (**a**) 143 cases and (**b**) selected 10 cases for MB006; (**c**) water rate matching results of 143 cases and (**d**) selected 10 cases for MB006.

In order to quantify the simulation results of cumulative gas and water production, the simulation deviation (SD) is defined as follows:

$$SD\% = \frac{Q_c - Q_o}{Q_o} \times 100\% \tag{3}$$

where $Q_c$ is the simulated cumulative production ($m^3$); $Q_o$ is the corresponding observed value ($m^3$).

The SD for gas ranges from −78.04% to 91.69%, averaging −2.65%. The SD for water ranges from −76.92% to 104.5%, averaging 1.3%. Due to the random combination of the selected seven sensitive parameters within their corresponding high and low bands, the variation ranges of SD values for gas and water are large. However, the small average SD values for gas and water indicate that the settings of the initial medium values for the seven sensitive parameters are reasonable.

### 5.2. Optimal Simulation Selection and EUR Prediction Method

The main aim of history matching is to attain a more accurate understanding of the geology by calibrating reservoir parameters to match the actual production data. In other words, the parameter combinations of the simulation cases having satisfied matching results are close to the actual geology conditions. In this study, two criteria, the SD range of −20% to 20% and trend matching of dynamic production, are used to distinguish the satisfied and unsatisfied simulation cases. According to these two criteria, the satisfied simulation cases are selected for MB005, MB006, and MB007, respectively. Then, the intersection of the aforementioned cases is determined. For this pilot area, ten optimal cases are finally selected (Figure 6b,d), and their parameter combinations are listed in Table 3. According to the absolute value of the average of SD, we classify the ten simulated cases and select the three best cases with less than 2% SD. Through this analysis, it is evident that the gas content, permeability, and fracture porosity are kept at their base values, with high Corey water. In other words, the initial settings of the aforementioned parameters are reasonable.

**Table 3.** Parameter settings for the top ten simulation cases.

| Case No. | Gas Content | VL | Permeability | Fracture Porosity | Corey Gas | Corey Water | Rock Compressibility | SD of Gas (%) MB005 | MB006 | MB007 | Average SD |
|---|---|---|---|---|---|---|---|---|---|---|---|
| 1 | Base | Base | Base | Medium | Low | High | Medium | 0.13 | 0.6 | −0.75 | −0.01 |
| 2 | Base | High | Base | Medium | Medium | High | Medium | 2.4 | 1.03 | 0.66 | 1.36 |
| 3 | Base | Base | Base | Medium | Medium | High | Low | − 1.85 | − 1.4 | − 0.92 | − 1.39 |
| 4 | Base | Low | Base | Medium | Medium | High | Medium | −2.56 | −2.15 | −1.7 | −2.13 |
| 5 | Base | Base | Base | Medium | Medium | Low | Medium | −3.55 | −2.53 | −1.16 | −2.41 |
| 6 | High | Base | Base | Medium | Medium | High | Low | 3.04 | 3.76 | 2.88 | 3.23 |
| 7 | Base | Base | Base | Low | Medium | High | Medium | −4.1 | −3.32 | −5.85 | −4.42 |
| 8 | Base | Base | High | Medium | Medium | High | Medium | 6.33 | 6.82 | 5.5 | 6.22 |
| 9 | Low | Base | Base | Medium | Medium | High | Medium | −9.76 | −9.52 | −10.25 | −9.84 |
| 10 | Base | High | Low | High | High | Low | Medium | 12.83 | 13.2 | 15.64 | 13.89 |

For all of these three wells, satisfied matching results are attained. In this paper, MB006 is selected as an example to illustrate this. Comparing the results from the top ten cases with the observed production data reveals a similarity between the simulated gas–water dynamic trend and the actual situation (Figure 6b,d). The SD of gas varies from −9.52% to 13.2%, as listed in Table 3.

Utilizing the top ten simulation cases, EUR predictions are conducted for these three wells with the constraint of BHFP. The initial pressure of each well in the dynamic model is set according to the actual value on the last production date. The target BHFP is set as 2 bar for each well after twenty years of dewatering.

## 6. Results and Discussion

### *6.1. EUR Prediction Results*

The EUR of the top ten cases is predicated for these three pilot wells. Taking the MB006 well as an example, all the cases show a similar trend, i.e., production initially increased, declined rapidly, and eventually stabilized later. The calculated EUR varies from $20.76 \times 10^6$ m$^3$ to $27.8 \times 10^6$ m$^3$, averaging $24.65 \times 10^6$ m$^3$ (Figure 7). Due to the scarce geological data and short production periods for these three pilot wells, it is hard to predict their future production accurately. However, the EUR ranges calculated by the top ten cases provide the EUR of individual wells with a high confidence degree.

### *6.2. Discussion*

#### 6.2.1. Application of Simulation Algorithms and Parameter Optimization

The central composite sampler algorithm used in this study is an experimental design algorithm to establish a quadratic surrogate model as an alternative algorithm to the Box–Behnken sampler. The central composite design includes embedded factors or fractional factor designs with a central point, enhanced by star points that facilitate estimating the model's response curvature. The number of star points is invariably double the number of factors, representing new extremes (low and high) for each factor in the design. Two types of support exist for the central composite design: inscribed and face-centered.

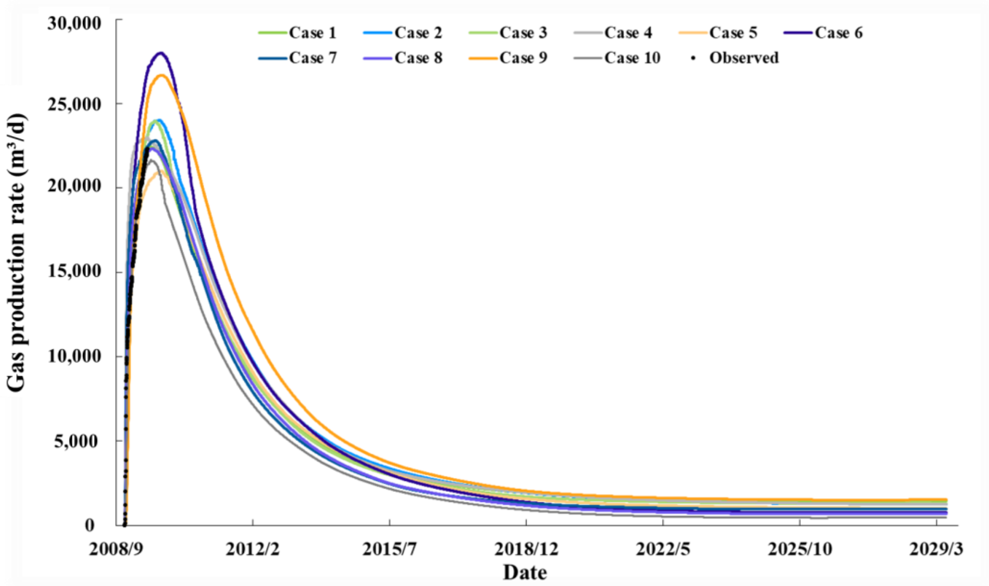


**Figure 7.** EUR forecast results of the top ten cases for MB006 well.

(1) **Inscribed type**

In this case, the central composite design represents a rotatable five-layer structure, where all off-center variables are positioned on the hypersphere within the factorial hypercube. In addition, in each dimension, these variables are consistently located on the hypersphere within the factorial hypercube (Figure 8a). This design yields high accuracy in the central space but exhibits reduced precision near the hypercube corners.

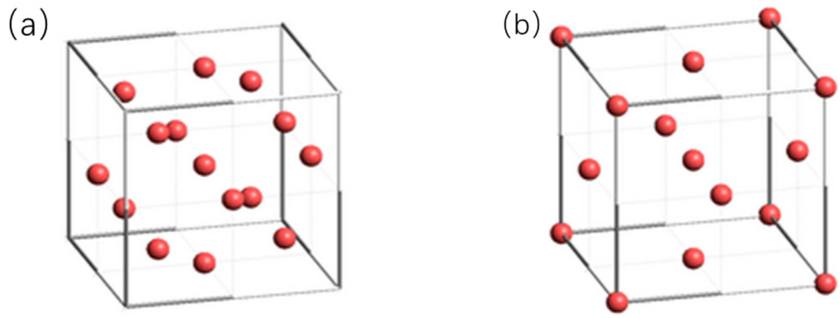


**Figure 8.** Center composite sampling type: (**a**) inscribed; (**b**) face-centered.

(2) **Face-centered type**

In this case, the central composite design in another scenario is a non-rotatable three-layer configuration, wherein all points diverging from the center reside on the factorial hypercube (Figure 8b). This arrangement signifies that the sequence of variables plays a critical role. It ensures commendable accuracy across the entire design space, albeit with marginally diminished precision in calculating pure quadratic coefficients.

This study selects seven parameters and generates 143 simulation cases using the face-centered algorithm of central composite sampling. Additionally, the number of parameters can be increased as the research requires the production of more matching cases, enhancing the representation of uncertainty. However, this approach is time-consuming; fewer parameters imply greater randomness. The seven reservoir parameters chosen for this study are notably representative, and the selected combination of simulation cases holds scientific significance.

#### 6.2.2. Analysis of Differences in Parameter Sensitivity

In this paper, the sensitivity analysis reveals that specific parameters, notably influential on gas and water production, have an SI value surpassing about 100%. For instance, gas content and permeability are critical for gas production, and fracture porosity and permeability are crucial for water production. These findings align with these of prior research [5,18,35]. However, the sensitivity degrees on gas and water production of other parameters are controversial [6,36–38] (Table 4). This may be because the high and low value setting approaches for the sensitivity parameters are different, e.g., empirical method, analogous method, testing data, or probability method. Given that the uncertainty ranges of the sensitivity parameters have an important impact on the simulated EUR for the pilot wells, the setting methods are pivotal for the CBM simulation task. The approach proposed in this paper is more reasonable and scientific.

**Table 4.** Previous studies on the sensitivity of various parameters.

| Authors | Sensitivity Parameters and Sequence | | | | | | | | |
|---|---|---|---|---|---|---|---|---|---|
| | **1** | **2** | **3** | **4** | **5** | **6** | **7** | **8** | **9** |
| Duan et al. [5] | Gc | K | Cg | VL | Φ | PL | Cw | C | Tau |
| Zhao et al. [18] | Gc | K | VL | Φ | Cw | Cg | Tau | C | |
| Acuna et al. [35] | Φ | Gc | K | Ng | Cg | | | | |
| Philpot et al. [36] | K | Xf | Φ | Gc | C | | | | |
| Zhou et al. [6] | K | VL | ρm | d | Φ | PL | Tau | | |
| Ru, T. [37] | Gc | Φ | K | d | | | | | |
| Liu et al. [38] | Gc | VL | K | S | Φ | | | | |

Note: Gc = gas content, K = permeability, Φ = fracture porosity, Cg = gas relative permeability, Cw = water relative permeability, VL = Langmuir volume, PL = Langmuir pressure, C = rock compression coefficient, Tau = desorption time, Xf = fracture half-length, ρm = coal density, d = coal thickness.

#### 6.2.3. Impact of Drilling Rate of Coal Seams on Gas Production

As shown in Figure 5a, the most sensitive parameters for gas production are gas content and permeability, which both are controlled by the burial depth. Considering the short well spacing of 100 m, the variation in geological properties in the pilot area should be not obvious. The peak production of the three wells is 18,259 $m^3/d$, 27,780 $m^3/d$, and 13,700 $m^3/d$, respectively. The obvious production performance difference may be due to the individual well drilling rate. As shown in Table 5, there is a positive correlation between the peak gas production and drilling rate of coal seam, which is consistent with the previous study [39]. The calculated P50 EUR of the individual wells also exhibits similar laws. In other words, in order to attain a decent production performance, the drill rate should be improved at the given horizontal length of the CBM well, and strategies may include conducting 3D seismic explanation or coal seam correlation before drilling.

**Table 5.** Drilling rates and P50 EUR for each pilot well.

| Well Name | Horizontal Length of the Well (m) | Horizontal Length in Coal (m) | Drilling Rate of Coal Seam (%) | Peak Gas Production ($m^3$/d) | P50 EUR ($m^3$) |
|---|---|---|---|---|---|
| MB005 | 632 | 546 | 86.4 | 18,259 | $11.4 \times 10^6$ |
| MB006 | 590 | 540 | 91.5 | 27,780 | $17.1 \times 10^6$ |
| MB007 | 586 | 480 | 81.9 | 13,700 | $8.0 \times 10^6$ |

#### 6.2.4. Comparison of EUR

There is a brown CBM field, the Moranbah gas field, in the Bowen Basin. The main developing well type is dual lateral SIS well, and the peak gas rate mainly varies from $30 \times 10^3$ $m^3/d$ to $60 \times 10^3$ $m^3/d$, with the EUR ranging from $14 \times 10^6$ $m^3$ to $30 \times 10^6$ $m^3$ [40]. In this pilot area, the average EUR of an individual well is about $12 \times 10^6$ $m^3$, which is almost a half less than that of the Moranbah gas field. Given that the drainage scope of the dual lateral SIS wells used in the Moranbah gas field is two times bigger than that of the single lateral SIS well used in the pilot areas, the individual EUR values are comparable (Figure 9). In other words, the simulated EUR in this paper is reliable and credible.

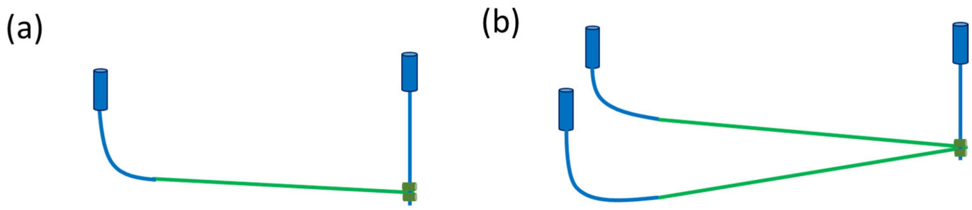


**Figure 9.** Well type of (**a**) single-lateral SIS and (**b**) dual-lateral SIS (the well trajectory indicated by light green color was completed with slotted liners).

The main reason for drilling a single lateral SIS well in this pilot area is to reduce costs. For this pilot area, if large-scale development planning is executed in the future, more well patterns should be used, such as a dual lateral SIS well, heel intersected lateral well, or standalone lateral well.

## 7. Conclusions

Considering challenges such as the absence of reservoir parameters and short period of production data in the C pilot area, this paper proposes a comprehensive numerical simulation method. This method not only incorporates comprehensive reservoir parameters but also considers the matching accuracy of both cumulative production and dynamic production trends when selecting optimal matching cases. The main conclusions are listed below:

(1) The distribution of gas content, permeability, VL, and PL exhibits a pattern that can be predicted by establishing their correlations with other parameters, respectively. In contrast, the distribution of fracture porosity, gas relative permeability, water relative permeability, rock compressibility, and sorption time does not show a discernible pattern.
(2) The gas production is most sensitive to gas content and permeability, and the water production is most sensitive to fracture porosity and permeability. So, the uncertainty range settings of these four parameters are pivotal for the simulated EUR.
(3) The ED method is an efficacious tool for analyzing parameter uncertainty, facilitating rapid history matching of production data, and identifying various combinations of CBM reservoir parameters, significantly reducing the time required for numerical simulation.
(4) A higher drilling rate of the coal seam corresponds to an increased peak gas production and a higher EUR of the pilot well. The simulated EUR of this pilot wells' values is comparable to that of the brown field in the Bowen Basin. In other words, the workflow to calculate EUR proposed in this paper is reliable and credible.

**Author Contributions:** Conceptualization, X.W.; methodology, X.W. and L.D.; software, L.D.; validation, L.D., S.Z. and S.T.; formal analysis, X.W.; investigation, S.Z.; resources, S.T.; data curation, X.W.; writing—original draft preparation, X.W.; writing—review and editing, L.D. and X.L.; visualization, J.L.; supervision, S.T.; project administration, S.T.; funding acquisition, L.D. All authors have read and agreed to the published version of the manuscript.

**Funding:** The project was financially supported by the National Natural Science Foundation of China: "Basic research on wettability and gas-water mobility of coal reservoirs", grant number 42272197.

**Data Availability Statement:** The research data of this article can be obtained from the corresponding author L.D. and S.Z. through reasonable requests.

**Conflicts of Interest:** The authors declare no conflicts of interest.

## References

1. Duan, L.J.; Xia, Z.H.; Qu, L.C.; Liu, L.L.; Wang, J.J. A new approach of history matching coalbed methane pilot wells. *Arab. J. Geosci.* **2019**, *12*, 526. [CrossRef]
2. Zou, M.J.; Wei, C.T.; Zhang, M.; Shen, J.; Shao, C.K. A mathematical approach investigating the production of effective water during coalbed methane well drainage. *Arab. J. Geosci.* **2014**, *7*, 1683–1692. [CrossRef]
3. Li, L.C.; Wei, C.T.; Qi, Y.; Cao, J.; Wang, K.Y.; Bao, Y. Coalbed methane reservoir formation history and its geological control at the Shuigonghe Syncline. *Arab. J. Geosci.* **2015**, *8*, 619–630. [CrossRef]
4. Ren, F.; Zhou, F.D.; Jeffries, M.; Beaney, S.; Sharma, V.; Lai, W.Q. Affecting Factors on History Matching Field-Level Coal Seam Gas Production from the Surat Basin, Australia. *Energy Fuel* **2024**, *38*, 3131–3147. [CrossRef]
5. Duan, L.J.; Zhou, F.D.; Xia, Z.H.; Qu, L.C.; Yi, J. New Integrated History Matching Approach for Vertical Coal Seam Gas Wells in the KN Field, Surat Basin, Australia. *Energy Fuel* **2020**, *34*, 15829–15842. [CrossRef]
6. Zhou, F.D. History matching and production prediction of a horizontal coalbed methane well. *J. Petrol. Sci. Eng.* **2012**, *96–97*, 22–36. [CrossRef]
7. Sang, H.T.; Sang, S.X.; Zhou, X.Z.; Liu, H.H.; Shi, W.; Zhang, K. Production History Fitting and Well Pattern Optimization in Coalbed Methane Well at Southern Part of Qinshui Basin. *J. Shandong Univ. Sci. Technol. Nat. Sci.* **2011**, *30*, 58–65. [CrossRef]
8. Zhang, Y.F.; Li, S.D.; Yue, P.; Duan, J.; Ning, W.; Wang, Z.B. Numerical simulation study on the effect of upper aquifer on coalbed methane development. *Unconv. Oil Gas* **2023**, *10*, 63–72. [CrossRef]
9. Gladys, C.; Aibassov, G. An Efficient Approach for History-Matching Coal Seam Gas CSG Wells Production. In Proceedings of the SPE Asia Pacific Oil and Gas Conference and Exhibition, Brisbane, Australia, 23–25 October 2018. [CrossRef]
10. Karacan, C.O. Production history matching to determine reservoir properties of important coal groups in the Upper Pottsville formation, Brookwood and Oak Grove fields, Black Warrior Basin, Alabama. *J. Nat. Gas. Sci. Eng.* **2013**, *10*, 51–67. [CrossRef]
11. Yang, J.S.; Liu, D.M.; Li, A.Q.; Xiao, Q.P.; Liu, L.T.; Cheng, D.S. Application of well-group numerical simulation in development of Qinshui CBM field. *Oil Drill. Prod. Technol.* **2010**, *32*, 103–106. [CrossRef]
12. Sawyer, D.N.; Cobb, W.M.; Stalkup, F.I.; Braun, P.H. Factorial Design Analysis of Wet-Combustion Drive. *Soc. Pet. Eng. J.* **1974**, *14*, 25–34. [CrossRef]
13. Peng, C.Y.; Gupta, R. Experimental Design in Deterministic Modelling: Assessing Significant Uncertainties. In Proceedings of the SPE Asia Pacific Oil and Gas Conference and Exhibition, Jakarta, Indonesia, 20–22 September 2003.
14. Corre, B.; Thore, P.; de Feraudy, V.; Vincent, G. Integrated Uncertainty Assessment for Project Evaluation and Risk Analysis. In Proceedings of the SPE European Petroleum Conference, Paris, France, 24–25 October 2000.
15. Peng, C.Y.; Gupta, R.; Vijayan, K.; Smith, G.C.; Rayfield, M.A.; DePledge, D.R. Experimental Design Methodology for Quantifying UR Distribution Curve—Lessons learnt and still to be learnt. In Proceedings of the SPE Asia Pacific Oil and Gas Conference and Exhibition, Perth, Australia, 18–20 October 2004.
16. Feraille, M.; Roggero, F.; Manceau, E. Application of Advanced History Matching Techniques to an Integrated Field Case Study. In Proceedings of the SPE Annual Technical Conference and Exhibition, Denver, CO, USA, 5–8 October 2003.
17. Alessio, L.; Coca, S.; Bourdon, L. Experimental Design as a Framework for Multiple Realisation History Matching: F6 Further Development Studies. In Proceedings of the SPE Asia Pacific Oil and Gas Conference and Exhibition, Jakarta, Indonesia, 5–7 April 2005.
18. Zhao, C.B.; Xia, Z.H.; Zheng, K.N.; Duan, L.J.; Liu, L.L.; Zhang, M.; Yang, Y. Integrated Assessment of Pilot Performance of Surface to In-Seam Wells to De-Risk and Quantify Subsurface Uncertainty for a Coalbed Methane Project: An Example from the Bowen Basin in Australia. In Proceedings of the SPE/EAGE European Unconventional Resources Conference and Exhibition, Vienna, Austria, 25–27 February 2014.
19. Peng, C.Y.; Gupta, R. Experimental Design and Analysis Methods in Multiple Deterministic Modelling for Quantifying Hydrocarbon In-Place Probability Distribution Curve. In Proceedings of the SPE Asia Pacific Conference on Integrated Modelling for Asset Management, Kuala Lumpur, Malaysia, 29–30 March 2004.
20. Van Elk, J.F.; Guerrera, L.; Vijayan, K.; Gupta, R. Improved Uncertainty Management in Field Development Studies through the Application of the Experimental Design Method to the Multiple Realisations Approach. In Proceedings of the SPE Asia Pacific Oil and Gas Conference and Exhibition, Brisbane, Australia, 16–18 October 2000.
21. Olivier, B.; Andrew, P.; Zach, C.; Doug, D. Geostatistical drillhole spacing analysis for coal resource classification in the Bowen Basin, Queensland. *Int. J. Coal Geol.* **2013**, *112*, 107–113. [CrossRef]
22. Li, M.; Kong, X.W.; Xia, Z.H.; Xia, M.J.; Wang, L.; Cui, Z.H.; Liu, L.L. Study on coalbed methane enrichment laws and exploration strategies in the Bowen Basin, Australia—A case of Moranbah coal measures in the Bowen block. *China Pet. Explor.* **2020**, *25*, 65–74.
23. Cui, Z.H.; Zhang, M.; Xia, Z.H.; Yang, Y.; Duan, L.J. Characteristics and potential evaluation of early permian blackwater group medium-rank coal in north Bowen basin of Australia. In Proceedings of the 2018 National Symposium on Coalbed Methane, Fuxin, China, 10–12 October 2018; p. 9.
24. Duan, L.J.; Qu, L.C.; Xia, Z.H.; Zhang, M.; Liu, L.L.; Zheng, K. Stochastic modeling of coalbed gas content: A case from Harcourt gas field of Bowen Basin, Australia. *Energy Sources Part. A Recovery Util. Environ. Eff.* **2019**, *41*, 1921–1927. [CrossRef]
25. Wang, X.M.; Zhang, Q.; Zhang, P.H. Discussion on the method of history matching of coalbed methane well. *Coal Geol. Explor.* **2003**, *31*, 20–22. [CrossRef]

26. Song, Y.; Liu, S.B.; Ju, Y.W.; Hong, F.; Jiang, L.; Ma, X.Z.; Wei, M.M. Coupling between gas content and permeability controlling enrichment zones of high abundance coal bed methane. *Acta Pet. Sin.* **2013**, *34*, 417–426. [CrossRef]
27. Kabir, A.; McCalmont, S.; Street, T.; Johnson, R., Jr. Reservoir Characterisation of Surat Basin Coal Seams using Drill Stem Tests. In Proceedings of the SPE Asia Pacific Oil and Gas Conference and Exhibition, Jakarta, Indonesia, 20–22 September 2011.
28. Clarkson, C.R.; Rahmanian, M.; Kantzas, A.; Morad, K. Relative permeability of CBM reservoirs: Controls on curve shape. *Int. J. Coal Geol.* **2011**, *88*, 204–217. [CrossRef]
29. Palmer, I. Permeability changes in coal: Analytical modeling. *Int. J. Coal Geol.* **2009**, *77*, 119–126. [CrossRef]
30. Ren, F.; Lei, G.; Arami-Niya, A.; Rufford, T.E.; Xing, H.; Rudolph, V. Gas storage potential and electrohydraulic discharge (EHD) stimulation of coal seam interburden from the Surat Basin. *Int. J. Coal Geol.* **2019**, *208*, 24–36. [CrossRef]
31. Young, G.B.C.; Paul, G.W.; McElhiney, J.E. A Parametric Analysis of Fruitland Coalbed Methane Reservoir Producibility. In Proceedings of the SPE Annual Technical Conference and Exhibition, Washington, DC, USA, 4–7 October 1992; pp. 461–473.
32. Liu, S.Q.; Sang, S.X.; Ma, J.S.; Yang, Y.H.; Wang, X.; Yang, Y.L. Analysis on gas and water output process of high rank coal reservoir in Southern Qinshui Basin. *Coal Sci. Technol.* **2017**, *45*, 1–6.
33. Wang, G.; Qin, Y.; Shen, J.; Zhao, L.J.; Zhao, J.C.; Li, Y.P. Experimental studies of deep low-rank coal reservoirs' permeability based on variable pore compressibility. *Acta Pet. Sin.* **2014**, *35*, 462–468. [CrossRef]
34. LI, J.M.; Liu, F.; Wang, H.Y.; Zhou, W.; Liu, H.L.; Zhao, Q.; Li, G.Z.; Wang, B. Desorption characteristics of coalbed methane reservoirs and affecting factors. *Pet. Explor. Dev.* **2008**, *35*, 52–58. [CrossRef]
35. Acuna, P.E.P.; Weatherstone, P.; Brett, P. Reservoir Modelling and Probabilistic Forecasting of the Walloons Coal Seam Gas Measures: Unique Challenges and Solutions to Regional CSG Reservoir Performance Prediction. In Proceedings of the SPE Asia Pacific Unconventional Resources Conference and Exhibition, Brisbane, Australia, 9–11 November 2015.
36. Philpot, J.A.; Mazumder, S.; Naicke, S.; Chang, G.; Boostani, M.; Tovar, M.; Sharma, V. Coalbed Methane Modelling Best Practices. In Proceedings of the International Petroleum Technology Conference, Beijing, China, 26–28 March 2013. [CrossRef]
37. Ru, T. Coal Reservoir Parameters Sensitivity Analysis Based on Numerical Simulation. *Coal Geol. China* **2017**, *29*, 31–34. [CrossRef]
38. Liu, S.G.; Peng, Z.G.; Wang, Z.B.; Chen, H.; Fu, Y. Numerical simulation of reservoir parameters influence on gas production in Qinshui Basin. *J. Liaoning Tech. Univ. (Nat. Sci. Ed.)* **2014**, *33*, 1302–1306.
39. Zhou, F.D.; Fernandes, G.; Luft, J.; Ma, K.; Oraby, M.; Guevara, M.O.; Kuznetsov, D.; Pinder, B.; Keogh, S. Impact of in-seam drilling performance on coal seam gas production and remaining gas distribution. *Appea J.* **2019**, *59*, 328. [CrossRef]
40. Hamilton, S.K.; Esterle, J.S.; Golding, S.D. Geological interpretation of gas content trends, Walloon Subgroup, eastern Surat Basin, Queensland, Australia. *Int. J. Coal Geol.* **2012**, *101*, 21–35. [CrossRef]


**Disclaimer/Publisher's Note:** The statements, opinions and data contained in all publications are solely those of the individual author(s) and contributor(s) and not of MDPI and/or the editor(s). MDPI and/or the editor(s) disclaim responsibility for any injury to people or property resulting from any ideas, methods, instructions or products referred to in the content.